Effective Mass-Squared Operators from Flavor Holonomy on a Compact Euclidean Four-Torus

Bled Workshop: Physics Beyond the Standard Models

Elia Dmitrieff

SI JAM Labs, Kazakhstan

July 2026

Under consideration in the Journal of Geometry and Physics (JGP)

Talk Architecture

Part I: Foundational Topology & Hydrodynamics

- The Empirical Challenge (NuFIT 6.0 vs. KATRIN)
- Critical Analysis of Conventional Mass Parameterization
- The Flat Euclidean T^4 Manifold Topology
- Emergent Minkowski Space-Time on Minimal Surfaces
- 3D Domain Walls & Stable Vacuum Isomers

Part II: Holonomy & Mass Generation (Next Segment)

- Localized Geometric Frustration & The Flavor Connection
- Modification of the Kaluza–Klein Momentum Spectrum
- The Non-Diagonal Effective Operator $\hat{M}^2_{\text{eff}}$
- Geometric Phase Differences vs. Fundamental Rest Mass
- Connection to Circulant Matrices & Jarlskog Invariant

The Empirical Flavor Landscape

- **Global Three-Flavor Fits (NuFIT 6.0 Paradigm):** Across solar, atmospheric, and reactor baselines, neutrino flavor transitions tightly constrain mass-squared splittings [1]:

$$\Delta m^2_{21} \approx 7.50 \times 10^{-5}\ \text{eV}^2, \quad |\Delta m^2_{31}| \approx 2.44 \times 10^{-3}\ \text{eV}^2 \tag{1}$$

- **Absolute Direct Mass Scales (KATRIN Kinematics):** Model-independent tracking of tritium beta-decay endpoints enforces an ultra-low direct upper boundary [2]:

$$m_{\nu_e} < 0.45\ \text{eV} \quad \text{(90\% C.L.)} \tag{2}$$

The Conceptual Risk of *Circulus in Definiendo*

Standard Quantum Field Theory automatically parameterizes these splittings by injecting explicit Dirac or Majorana mass terms into the electroweak Lagrangian. **The Trap:** Assuming that an observed $\Delta m^2 \neq 0$ *syntactically requires* a fundamental, non-zero rest mass parameter.

The Core Thesis: Massless Emergence

The Alternative Framework

We present a unified hydro-topological architecture where:

- **Complete Absence of Bare Masses:** All active neutrinos remain structurally massless ($m_{\mathrm{bare}} = 0$).
- **No Fundamental Mass Insertions:** Neither Dirac nor Majorana mass terms are utilized.
- **Geometric Origin:** Neutrino flavor oscillations are governed completely by **flavor holonomy** and spatial compactification metrics.

Observed physical parameters shift from fundamental coupling constants to topological invariants.

The Fundamental Manifold Geometry (T^4)

Let the background micro-structure of the vacuum be defined on a flat Euclidean four-torus:

$$T^4 = \mathbb{R}^4/\Lambda \tag{3}$$

Coordinate Anatomy

- **3 Extended Directions:** $\mathbf{x} = (x, y, z)$ corresponding to large macroscopic spaces.
- **1 Highly Compact Cycle:** A periodic, microscopic spatial coordinate w bounded by circumference L_w:

$$w \sim w + L_w \tag{4}$$

Crucial Distinction Regarding w

The compact coordinate w is **not** identified with physical time. Minkowski space-time is strictly an emergent, low-energy hydrodynamic description restricted to a geometric hypersurface.

Why a Toroidal Topology?

Elimination of Boundary Artifacts:

- Open boundaries or boundary defects in a Euclidean vacuum lattice inject massive large-scale geometrical distortions.
- Global compactification via $\mathbb{R}^4/\Lambda$ isolates a perfectly homogeneous background geometry.
- Provides a highly stable substrate for a continuous hydrodynamic vacuum state.

Microscopic Substrate

The global torus topology allows unperturbed periodic structures to establish smooth, uniform continuous flow equations without edge localized singularities.

The 3D Minimal-Surface Domain Wall

- Consider a **3D minimal-surface domain wall** acting as a boundary phase (0).
- This hypersurface cleanly separates two stable 4D bulk domains, designated as phase $(+)$ and phase $(-)$.

Hydrodynamic Boundary Conditions

A fundamental 4D quasi-liquid substance fills the bulk, governed by the continuous, incompressible flow condition:

$$\nabla \cdot \vec{v}_{4D} = 0 \tag{5}$$

To maintain global structural stability, the fluid flow vectors must be **strictly tangential** to the 3D domain wall.

The Instability of Normal Flow

Any normal velocity component $(\vec{v} \cdot \hat{n} \neq 0)$ across the interface forces a macroscopic hypersurface drift. This absorption of the alternating bulk phases $(\pm)$ would instantly destabilize the physical vacuum structure.

Spacetime Emergence and Flow Modes on the Domain Wall

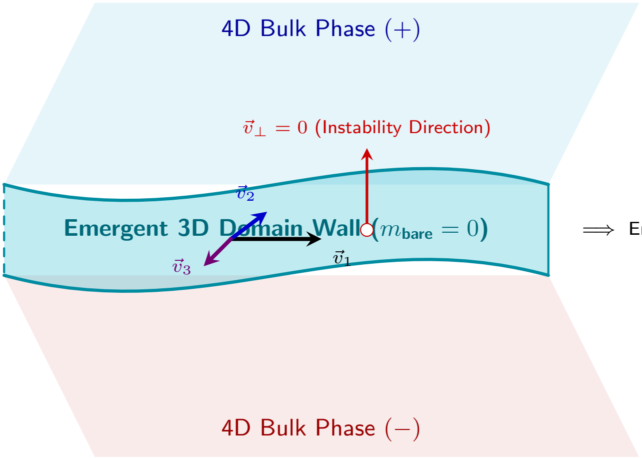

$\Longrightarrow$ Emergent Minkowski Spacetime

Figure: Spacetime Emergence and Flow Modes on the Domain Wall

Generation of Three Discrete Active Flavors

Bounding the continuous, incompressible fluid parallel to the periodic grid geometry of the domain wall within a compact torus restricts global continuity to exactly **three discrete, orthogonal flow modes**:

$$\mathcal{B}_{\mathrm{flow}} = \{\vec{v}_1, \vec{v}_2, \vec{v}_3\} \tag{6}$$

Physical Features of the Flow Modes

- These modes represent alternative topological configurations of the underlying fluid background.
- They cause *zero deformation* to the wall's global geometry.
- **Conclusion:** They manifest as structurally massless vacuum isomers ($m_{\text{bare}} = 0$).

The Mixing Context

The standard unitary mixing matrix U functions as the change-of-basis engine, mapping these weak-interaction hydrodynamic flavor modes to the actual propagation eigenstates.

Geometric Intuition: The “Satori” Polytope Framework

- **The Microscopic Origin:** A candidate realization for this discrete 3-mode distribution stems from the author’s recently proposed four-dimensional space-filling **“Satori” polytope construction** [6].
- **Chiral Interfaces:** The elementary translational cell inside the Satori network features a distinct chiral configuration of open 3D interfaces.
- **Symmetry Motivation:** This geometric layout naturally isolates and supports exactly three distinct, stable tangential circulation patterns.

Independence of the Present Model

While the Satori tessellation provides elegant geometric motivation for the existence of three stable hydrodynamic modes, the analytical results derived here rely solely on the general topology of the domain-wall flow constraints.

The Standard Translation Benchmark

- **Infinitesimal Spatial Shifts:** In standard quantum mechanics, an infinitesimal transformation of a field spatial profile $\Psi(w)$ by a distance ϵ along the coordinate w is generated by the momentum operator $\hat{p}_w = -i\hbar\partial_w$.
- **Finite Translation Operator:** The finite translation operator $\hat{T}(\epsilon)$ is defined conventionally as:

$$\hat{T}(\epsilon)\Psi(w) = \exp\left(\epsilon\frac{\partial}{\partial w}\right)\Psi(w) = \Psi(w+\epsilon) \tag{7}$$

Standard Periodic Boundary Conditions

Under unfrustrated periodic boundary conditions $\Psi(w) = \Psi(w + L_w)$, this operator maps the state smoothly around the cyclic loop without altering its kinetic energy eigenvalues.

The Shifted Translation Operator & Flavor Connection

Tangential transport along a curved or frustrated wall changes the orientation of the local circulation basis. Since flavor labels correspond directly to circulation modes, parallel transport acts non-trivially on the flavor vector space.

The Infinitesimal Transport Generator

The transport is governed by an anti-Hermitian connection Γ_w, satisfying:

$$\Gamma_w^\dagger = -\Gamma_w \quad \Longrightarrow \quad \Gamma_w = i\lambda_0 \tag{8}$$

where λ_0 is a strictly Hermitian flavor-space matrix.

The Covariant Transport Engine

The ordinary derivative is replaced by the flavor covariant derivative:

$$D_w = \frac{\partial}{\partial w} + i\lambda_0 \tag{9}$$

Characterizing the Flavor Holonomy

The physically observable quantity characterizing flavor transport around the compact cycle is the holonomy operator W:

$$W = P \exp\left(\oint D_w \, dw\right) \tag{10}$$

Analytical Strategy for this Framework

- The presentation restricts attention to the corresponding local connection $\Gamma_w = i\lambda_0$.
- The spectrum of λ_0 uniquely determines the effective low-energy oscillation parameters.
- Distinct circulation patterns acquire distinct geometric phases when transported around the compact cycle.

Result: Observable oscillation frequencies emerge without introducing fundamental Dirac or Majorana mass parameters.

The Flavor Holonomy Phase Shift Loop

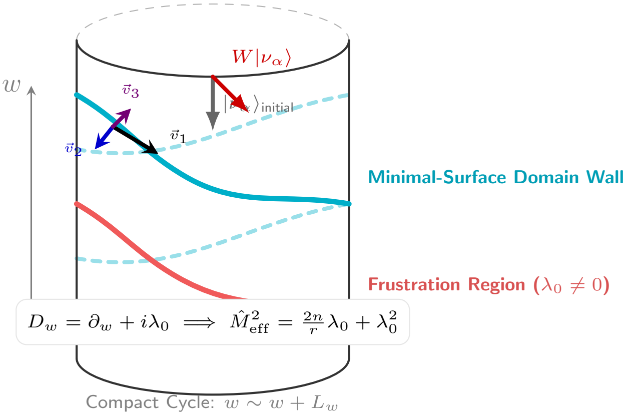

Figure: The Flavor Holonomy Phase Shift Loop

Kaluza–Klein Decomposition on T^4

The compact coordinate w admits a traditional Kaluza–Klein expansion [7][8]:

$$\Psi(x, w) = \sum_n \psi_n(x) e^{inw/r} \tag{11}$$

where the compactification radius r is given by:

$$r = \frac{L_w}{2\pi} \tag{12}$$

Action of the Flavor Covariant Derivative

Applying the covariant derivative $D_w = \frac{\partial}{\partial w} + i\lambda_0$ directly to a specific KK winding mode yields:

$$D_w \Psi = i\left(\frac{n}{r} + \lambda_0\right)\Psi \tag{13}$$

Isolating the Winding Spectrum

Squaring the covariant derivative operator establishes the geometric kinetic energy infrastructure:

$$-D_w^2 \Psi = \left(\frac{n}{r} + \lambda_0\right)^2 \Psi \tag{14}$$

The KK Mass-Squared Operator

The operator associated with propagation around the compact cycle is thus:

$$\hat{M}_{\mathrm{KK}}^2 = \left(\frac{n}{r} + \lambda_0\right)^2 \tag{15}$$

Expanding the square yields:

$$\hat{M}_{\mathrm{KK}}^2 = \frac{n^2}{r^2}\mathbf{1} + \frac{2n}{r}\lambda_0 + \lambda_0^2 \tag{16}$$

The Background Absorption Mechanism

$$\hat{M}_{\mathrm{KK}}^2 = \underbrace{\frac{n^2}{r^2}\mathbf{1}}_{\text{Universal Background}} + \frac{2n}{r}\lambda_0 + \lambda_0^2 \tag{17}$$

The Universal Background Filtering

- The first term $(\frac{n^2}{r^2}\mathbf{1})$ is entirely flavor-independent.
- It represents the universal background Kaluza–Klein contribution shared by all hydrodynamic modes.
- Neutrino oscillation observables depend *only* on relative phase differences between propagation eigenstates.
- **Action:** This common term can be absorbed into the unperturbed vacuum background associated with the compactified dimension.

The Emergent Mass-Squared Operator

Subtracting the universal background contribution isolates the true low-energy effective operator:

$$\hat{M}^2_{\text{eff}} = \hat{M}^2_{\text{KK}} - \frac{n^2}{r^2}\mathbf{1} \tag{18}$$

The Core Operator Formula

$$\boxed{\hat{M}^2_{\text{eff}} = \frac{2n}{r}\lambda_0 + \lambda_0^2} \tag{19}$$

For the lowest non-trivial winding sector $(n = 1)$, the equation reduces to:

$$\hat{M}^2_{\text{eff}} = \frac{2}{r}\lambda_0 + \lambda_0^2 \tag{20}$$

Linearization and Mass-Squared Splittings

Assuming that the eigenvalues λ_i of the connection matrix are small relative to the compactification scale:

$$|\lambda_i| \ll \frac{2}{r} \tag{21}$$

The Linearized Splitting Formula

The effective physical mass-squared splittings simplify linearly to:

$$\Delta m_{ij}^2 \approx \frac{2}{r}(\lambda_i - \lambda_j) \tag{22}$$

Physical Interpretation

The experimentally observed oscillation scales are generated by **differences in flavor holonomy** around the compact cycle rather than by fundamental rest masses. Only flavor-dependent deviations from the vacuum background enter the effective low-energy spectrum.

Theoretical Affiliations & Paradigm Comparison

Deep Conceptual Analogies

The mathematical architecture is fundamentally linked to well-established geometric concepts:

- **Berry Phase Phenomenology:** Geometric phases in adiabatic cycles [9].
- **Wilson-Loop Observables:** Gauge-invariant non-local field variables [10].
- **Hosotani Mechanism:** Dynamic symmetry breaking via gauge holonomies on compact cycles [11].

Crucial Structural Divergence

Unlike the Hosotani mechanism or standard gauge theories:

- This connection is **not** a gauge field originating from an internal gauge symmetry.
- It is an **effective flavor connection** generated entirely by hydrodynamic transport along the microscopic domain-wall network geometry.

Evolution of the Fluid Superposition

Let a neutrino be produced at $x = 0$ in a pure weak flavor state $|\nu_\alpha\rangle$. It evolves as a linear superposition of stable global fluid modes $|\nu_i\rangle$:

$$|\nu_\alpha\rangle = \sum_i U^*_{\alpha i} |\nu_i\rangle \tag{23}$$

Space-Time Phase Propagation

The phase evolution of each individual fluid mode is strictly governed by its corresponding effective mass-squared eigenvalue $M^2_{i,\text{eff}}$:

$$|\nu_i(t)\rangle = \exp\left(-iE_i t + ip_i x\right)|\nu_i\rangle \tag{24}$$

Applying the ultra-relativistic approximation for a shared momentum $p \approx E$:

$$E_i = \sqrt{p^2 + M^2_{i,\text{eff}}} \approx p + \frac{M^2_{i,\text{eff}}}{2E} \tag{25}$$

Isolating the Geometric Transition Amplitude

Substituting the macroscopic path length relation $x \approx t \approx L$ into the relative phase difference between alternative fluid modes i and j isolates the geometric phase engine:

$$\Delta\phi_{ij} = \frac{\Delta M^2_{ij,\text{eff}}}{2E} L = \frac{(\lambda_i - \lambda_j)L}{r \cdot E} \tag{26}$$

Transition Probability Equation

The projection into an alternate weak flavor state $|\nu_\beta\rangle$ is formulated as:

$$P_{\nu_\alpha \to \nu_\beta} = \left| \sum_i U_{\beta i} U^*_{\alpha i} \exp\left(-i \frac{M^2_{i,\text{eff}} L}{2E} \right) \right|^2 \tag{27}$$

The Geometric Oscillation Master Formula

Expanding the modulus squared yields the standard kinematic oscillation profile:

$$\begin{aligned} P_{\nu_\alpha \to \nu_\beta} = \delta_{\alpha\beta} &- 4 \sum_{i>j} \mathsf{Re}(U_{\beta i} U^*_{\alpha i} U^*_{\beta j} U_{\alpha j}) \sin^2\left(\frac{\Delta\lambda_{ij} L}{2rE}\right) \\ &+ 2 \sum_{i>j} \mathsf{Im}(U_{\beta i} U^*_{\alpha i} U^*_{\beta j} U_{\alpha j}) \sin\left(\frac{\Delta\lambda_{ij} L}{rE}\right) \end{aligned} \tag{28}$$

Core Physical Verification

- The standard empirical oscillation length is recovered **exactly**.
- Crucially, the transformation utilizes the **geometric parameters of the torus (r)** and flavor connection steps ($\Delta\lambda_{ij}$) rather than a fundamental bare mass insertion.

The Geometrical Link to Circulant & Democratic Textures

How does the flavor connection matrix λ_0 interact with discrete flavor symmetries?

The Circulant-Democratic Baseline

If the 3-mode hydrodynamic flow along the Satori polytope has unperturbed cyclic permutation symmetry, λ_0 is a **circulant matrix**. A special boundary case is the **democratic texture** $(c_0 = c_1 = c_2 = c)$:

$$\lambda_0^{\text{circulant}} = \begin{pmatrix} c_0 & c_1 & c_2 \\ c_2 & c_0 & c_1 \\ c_1 & c_2 & c_0 \end{pmatrix} \xrightarrow{\text{Democratic}} \lambda_0^{\text{dem}} = c \begin{pmatrix} 1 & 1 & 1 \\ 1 & 1 & 1 \\ 1 & 1 & 1 \end{pmatrix} \tag{29}$$

Both matrices are universally diagonalized by the Discrete Fourier Transform matrix F_3, shifting the framework into a purely geometric mixing baseline (e.g., tribimaximal structures [4]).

Geometric Frustration vs. The Jarlskog Invariant

Geometric Frustration vs. The Jarlskog Invariant (J)

The imaginary component of our master oscillation formula maps to the **Jarlskog invariant** (J) [5]:

$$\mathrm{Im}(U_{\beta i}U^*_{\alpha i}U^*_{\beta j}U_{\alpha j}) \equiv \pm J \tag{30}$$

- **The Symmetric Limit:** Under perfect circulant or democratic geometry, $J = 0$ (zero CP violation).
- **The Frustration Mechanism:** Non-zero CP violation ($J \neq 0$) is generated dynamically when localized **geometric frustration** perturbatively breaks this circular/democratic symmetry.

Connection to the Bled Paradigm: Parameter Reduction

Top-Down Phenomenological Fit

As investigated by **Kleppe (2025)** [3]:

- Traditional models use nearly democratic mass matrices to describe the flavor sector.
- The Jarlskog invariant is imposed as a strict top-down constraint to successfully reduce the number of free parameters from 6 to 5.
- It remains an open question *why* nature selects these parameter-restricted textures.

Our Bottom-Up Geometric Origin

Our hydro-topological T^4 model provides the underlying physical mechanism:

- The vanishing of J is a fundamental geometric rule of an unperturbed cyclic vacuum lattice.
- Parameter reduction is not an accidental field-theoretic choice, but a topological consequence.
- Measurable CP violation becomes a direct, physical readout of the **structural distortion** of the domain walls.

This unifies algebraic texture constraints with the spatial geometry of the compact cycle.

Core Findings

The Paradigm Shift

- Non-zero effective mass-squared splittings (Δm^2) can be derived **without** a fundamental bare rest mass parameter ($m_{\text{bare}} = 0$).
- Explicit Dirac or Majorana mass terms are entirely replaced by the eigenvalues of a **flavor connection matrix (λ_0)** operating on a compactified torus (T^4).
- Oscillations represent the manifestation of **flavor-dependent holonomy** generated by tangential hydrodynamic transport.

Physical metrics transform seamlessly from fundamental coupling parameters into topological invariants.

Future Roadmaps for the Model

1. **Microscopic Derivation:** Compute the precise configuration of λ_0 straight from the domain wall's curvature, branching layouts, and defect interactions.
2. **Fluid Stress-Energy Tensor:** Formulate the explicit 4D hydrodynamic stress tensor to mathematically guarantee the unique isolation of exactly three discrete flow modes.
3. **Emergent Gravitation:** Investigate if large-scale collective distortions of the domain-wall boundary induced by defect populations can mimic an effective spacetime metric.
4. **Topological Charge Mapping:** Establish exact algebraic mappings between the Euler characteristic (χ) of the manifold and standard integer/fractional field charges $(0, \pm 1/3, \pm 2/3, \pm 1)$.
5. **Chiral Weak Interactions:** Trace the structural handedness of the Satori tessellation to explain the maximal parity violation observed in active neutrino interactions.

References I

- Esteban, I., et al. "NuFit-6.0: Updated global analysis of three-flavor neutrino oscillations," *JHEP* 12 (2024) 216.
- Aker, M., et al. (KATRIN Collaboration). "Direct neutrino-mass measurement based on 259 days of KATRIN data," *Science* 388 (2025).
- Kleppe, A. "On CP-violation and quark masses: reducing the number of free parameters," *arXiv preprint* arXiv:2508.11081 (2025).
- Harrison, P. F., Perkins, D. H., & Scott, W. G. "Tri-bimaximal mixing and the neutrino paradox," *Phys. Lett. B* 530 (2002) 167.
- Jarlskog, C. "A Basis-Independent Formulation of Flavor Mixing and CP Nonconservation," *Z. Phys. C* 29 (1985) 491.
- Dmitrieff, E. G. "Tessellation Approach in Modeling Properties of Physical Vacuum," 22nd Bled Workshop (2019) 190–203.
- Kaluza, T. "Zum Unitätsproblem der Physik," Sitzungsber. Preuss. Akad. Wiss. Berlin (1921) 966.
- Klein, O. "Quantum Theory and Five-Dimensional Relativity," Z. Phys. 37 (1926) 895.
- Berry, M.V. "Quantal Phase Factors Accompanying Adiabatic Changes," Proc. Roy. Soc. Lond. A392 (1984) 45.
- Wilson, K.G. "Confinement of Quarks," Phys. Rev. D10 (1974) 2445.
- Hosotani, Y. "Dynamical Mass Generation by Compact Extra Dimensions," Phys. Lett. B126 (1983) 309.
- Hosotani, Y. "Dynamics of Nonintegrable Phases," Ann. Phys. 190 (1989) 233.